MultiCraft

International Journal of Engineering, Science and Technology
Vol. 11, No. 4, 2019, pp. 10-22

INTERNATIONAL JOURNAL OF ENGINEERING, SCIENCE AND TECHNOLOGY

www.ijest-ng.com
www.ajol.info/index.php/ijest

Detection and classification of four phase to ground faults in a 138 kV six phase transmission line using Hilbert Huang transform

Gaurav Kapoor

Department of Electrical Engineering, Modi Institute of Technology, Kota, Rajasthan, INDIA
Corresponding Author: e-mail: gaurav.kapoor019@gmail.com, Mobile: +91-9166868988

Abstract

In this work, the Hilbert Huang transform (HHT) is used for the detection and classification of four phase to ground faults in the six-phase transmission line (SPTL). Using the HHT, the faults can be detected, classified and the faulted phase can be recognized merely, by calculating the amplitudes of HHT coefficients of six-phase fault currents. HHT is utilized for extracting the features of the six-phase fault currents recorded at one end only. The HHT is extensively tested using the MATLAB model of 138 kV, 60 Hz, and 68 km long SPTL. The possibility of HHT is investigated under extensive variations of the fault factors. The results exemplify that the HHT effectively detects and categorizes all types of four phase to ground faults regardless of varying the fault factors.

Keywords: Fault detection, fault classification, faulty phase recognition, Hilbert Huang transform, six phase transmission line.

DOI: http://dx.doi.org/10.4314/ijest.v11i4.2

1. Introduction

The possibility of fault occurrence on the six-phase transmission line is more when comparing with the double circuit transmission lines. Thus, exact detection of the faults in the six-phase transmission line turns out to be very influential for extenuating the loss of gain and providing rapid renovates.

Quite a few newly reported research studies addressed the issues related to fault recognition and categorization in six-phase transmission line. Some important research attempts are presented in brief in this section. In (Gautam *et al*., 2018), wavelet transform has been used for fault detection in series capacitor compensated double circuit transmission line. Wavelet transform based fault detection and classification tool has been proposed for the protection of a 400 kV double circuit transmission line (Gautam *et al*., 2018). A back-up protection technique has been presented in (Jena *et al*., 2017) for the series capacitor compensated transmission line. Detection and recognition of multi-position three phase to ground faults in a twelve phase transmission line using wavelet transform has been presented in (Kapoor, 2018). Wavelet transform based detection of far-end and near-in faults in six-phase transmission line has been reported in (Kapoor, 2018). Phase to phase faults detection in a series capacitor compensated six-phase transmission line using wavelet transform has been proposed in (Kapoor, 2018). In (Kapoor, 2018), mathematical morphology has been used for the detection of far-end and near-in faults. Hilbert Huang transform has been applied for the detection and classification of single line to ground near-in and far-end faults in a 138 kV six-phase transmission line (Kapoor, 2019). In (Kapoor, 2019), discrete Walsh Hadamard transform has been used for the protection of wind farm integrated series capacitor compensated three phase transmission line. A protection scheme based on discrete wavelet transform has been presented in (Kapoor, 2018) for a twelve phase series capacitor compensated transmission line. In (Kapoor, 2018), a fault detector based on wavelet transform has been proposed for series capacitor compensated three phase transmission line. In (Koley *et al*., 2015), wavelet transform in conjunction with artificial neural network has been applied for the protection of six-phase transmission line. Sharma *et al*., 2017 used mathematical morphology for the protection of boundary of a six-phase transmission line. Walsh Hadamard transform has been used for fault detection in series capacitor compensated transmission line (Sharma *et al*.,

2018). Hilbert Huang transform has been applied for the detection of faults in a wind farm integrated series capacitor compensated transmission line (Sharma *et al*., 2018).

In this work, the Hilbert Huang transform (HHT) is executed for the detection and classification of four phase to ground faults in a six-phase transmission line. Such type of research has not been depicted so far to the best of the information of the author. The results illustrates that the HHT competently detects the faults, and the uniformity of the HHT is not susceptible to the deviations in the fault factors.

This article is structured as: Section 2 presents the specifications of six-phase transmission line. Section 3 describes the process for fault detection using HHT. Section 4 reports the performance appraisal of the investigations carried out in this work. Section 5 concludes the article.

2. The Specifications of Six-Phase Power Transmission System

Figure 1 shows the schematic of six-phase power transmission system. The power transmission system consists of a 138 kV, 60 Hz, 68 km long six-phase transmission line which is divided into two zones. Each zone has a length of 34 km. The six-phase transmission line is fed from a 138 kV source at the sending and at the receiving end. The two loads of 300 MW and 150 MVAr are connected at the receiving end of a six-phase transmission line. The model of six-phase transmission line is developed and simulated using the simscape power system toolbox of MATLAB.

As shown in Figure 1, the current measurements blocks for the relay are connected at bus-1 to protect the entire length of six-phase transmission line. Figure 2 shows the six-phase current and voltage waveforms for no-fault. Figure 3 depicts the Hilbert Huang coefficients of six-phase currents for no-fault. Table 1 reports the response of the HHT for no-fault condition.

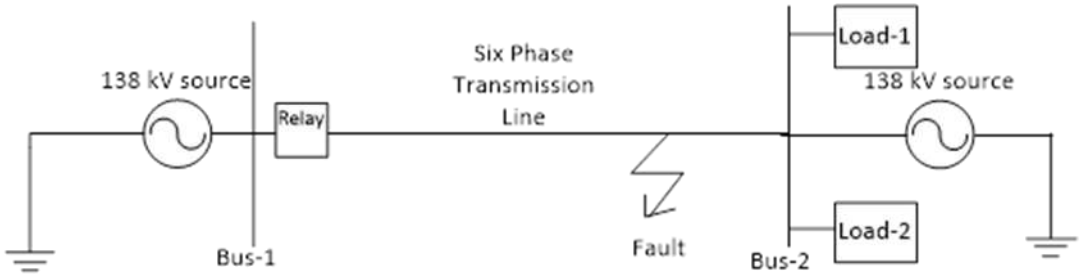

Figure 1. The schematic of proposed simulation model

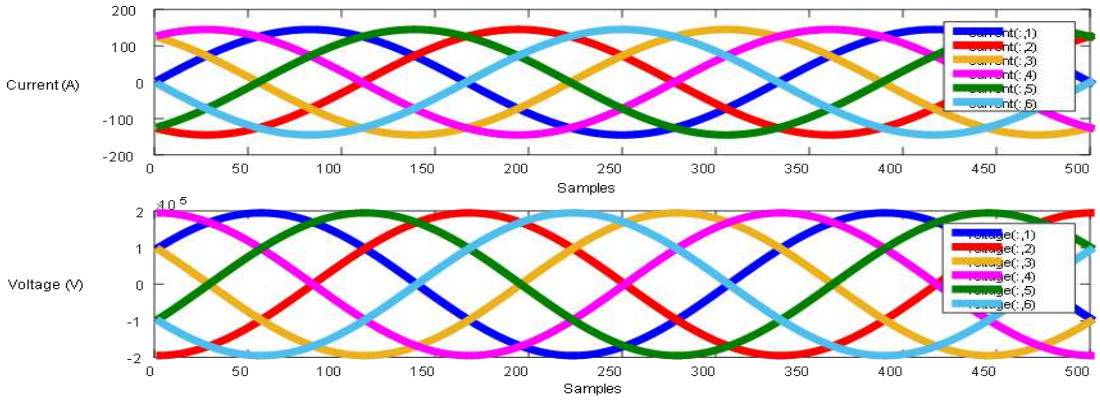

Figure 2. Six phase current and voltage waveforms for no-fault

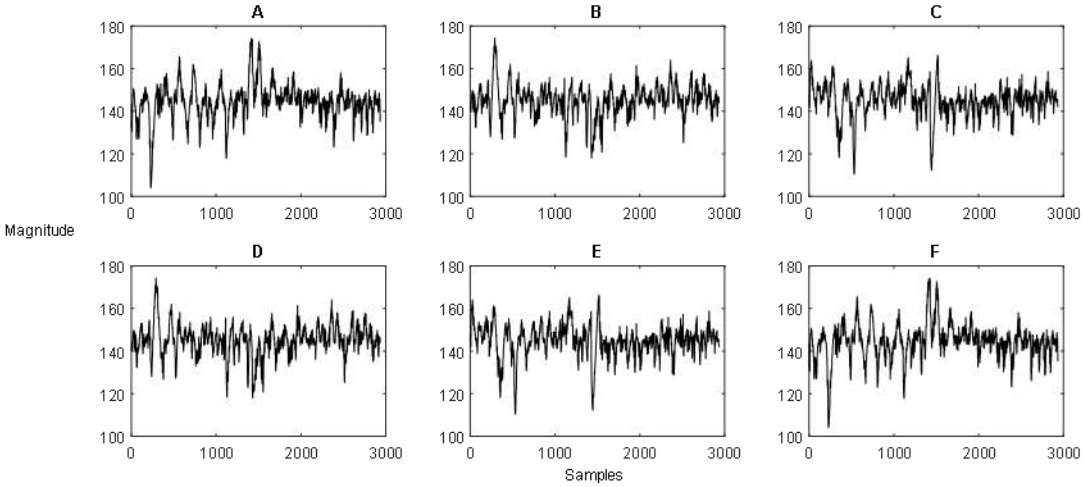

Figure 3. HHT coefficients of six phase current for no-fault

Table 1. Result for no-fault

Phase	Hilbert Huang Transform Coefficients
A	174.2376
B	174.3952
C	166.3926
D	174.4135
E	166.3862
F	174.2411

3. The Hilbert Huang Transform Based Fault Detection Technique

The Hilbert transform for a test signal f (t) is defined as given in equation-1 below (Sharma *et al*., 2018):

$$H\{f(t)\} = -\frac{1}{\pi}\int_{-\infty}^{\infty} f(\tau)\frac{d\tau}{\tau - t} = -\frac{1}{\pi t} * f(t) \tag{1}$$

Hilbert transform can be defined as the convolution between f(t) and -1/πt.

This equation defines an inappropriate integral, because for t = τ the integral has an exceptionality. So the integral is calculated symmetrically to avoid this difficulty.

$$\int_{-\infty}^{\infty}\frac{g(\tau)}{t-\tau}d\tau = \lim_{e\to 0}\left[\int_{-\infty}^{t-e}\frac{g(\tau)}{t-\tau}d\tau + \int_{t+e}^{\infty}\frac{g(\tau)}{t-\tau}d\tau\right] \tag{2}$$

Inverse Hilbert transform can be deliberated by equation-3, where g' (t) and g (t) are part of pair transform of Hilbert (Kapoor, 2019).

$$g(t) = -\frac{1}{\pi}\int_{-\infty}^{\infty}\frac{g'(t)}{t-\tau} * d\tau \tag{3}$$

From the definition of Hilbert Transform it is observed that g' (t) can be understood as the convolution of g (t) with the signal -1/πt.

$$g'(t) = g(t) * \frac{1}{\pi t} \tag{4}$$

Figure 4 shows the process of Hilbert Huang transform for fault detection and classification. The steps for the same are shown below.

Step 1 Simulate the model for different four phase to ground faults and generate the six-phase fault current signals.

Step 2 Analyze the six-phase currents using Hilbert Huang transform for the removal of their characteristics.

Step 3 Calculate the amplitudes of HHT coefficients for each fault current signal.
Step 4 The phase will be declared as the faulted phase if its HHT coefficient has the larger amplitude in comparison to the healthy phase.

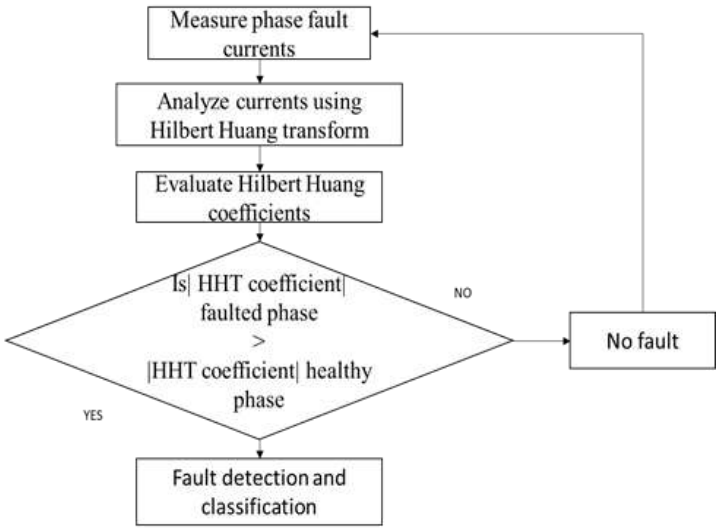

Figure 4. HHT procedure for fault detection and classification

4. Results and Discussions

The efficacy of Hilbert Huang transform has been tested for various types of four phase to ground faults. The fault factors of the simulation model are varied in each case. The results are shown in the subsequent subsections.

4.1 Performance in Case of ACDFG Fault: The performance of HHT is evaluated for ACDFG four phase to ground fault triggered at 34 km away from the relaying point at fault triggering time of 0.05 seconds with $R_F = 2\ \Omega$ and $R_G = 4\ \Omega$. Figure 5 demonstrates the waveform of six phase current for ACDFG fault. Figure 6 depicts the Hilbert Huang transform coefficients of six phase current for ACDFG fault. Table 2 reports the response of HHT for ACDFG fault. It is examined from Table 2 that the amplitudes of Hilbert Huang coefficients of the faulted phases are greater than the amplitudes of Hilbert Huang coefficients of the healthy phases. Thus, the HHT correctly detects the ACDFG fault.

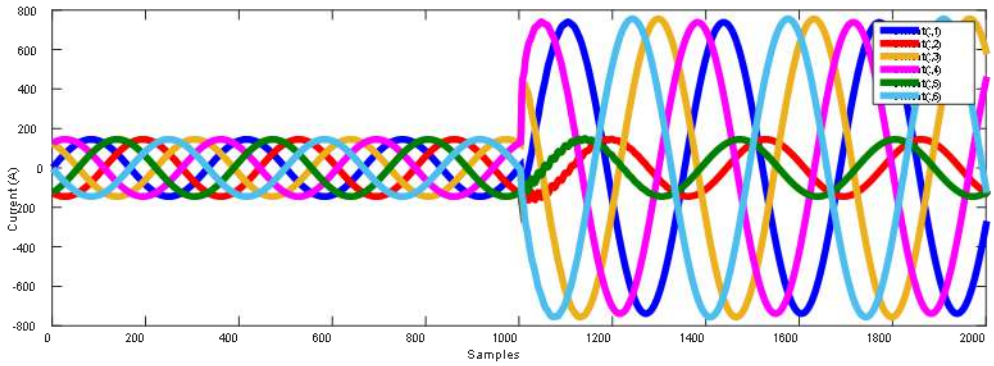

Figure 5. Six phase current for ACDFG fault at FIT=0.05 seconds with $R_F = 2\ \Omega$ and $R_G = 4\ \Omega$

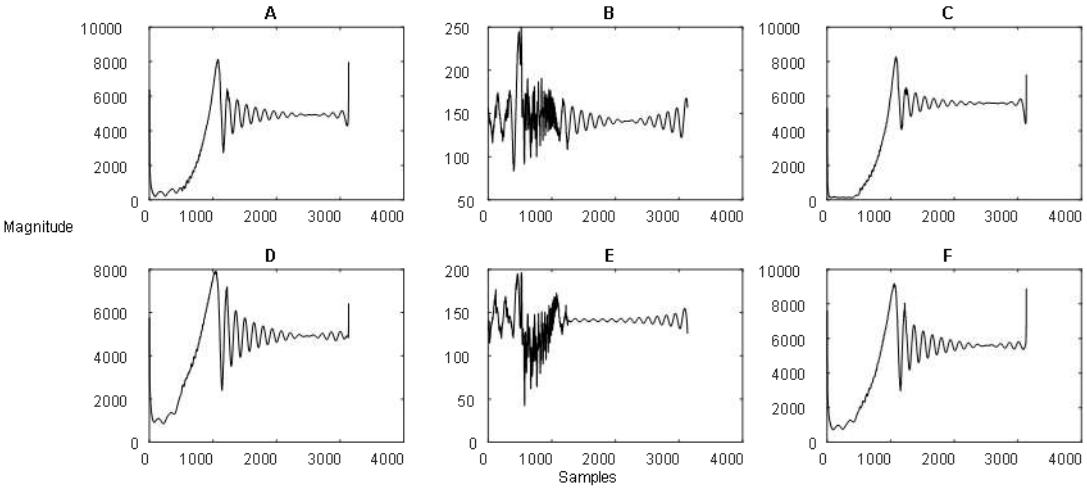

Figure 6. HHT coefficients of six phase current for ACDFG fault at FIT=0.05 seconds with R_F = 2 Ω and R_G = 4 Ω

Table 2. Result for ACDFG fault at 34 km at FIT = 0.05 seconds with R_F = 2 Ω and R_G = 4 Ω

Phase	Hilbert Huang Transform Coefficients
A	8.1225*10^3
B	249.8865
C	8.2842*10^3
D	7.9265*10^3
E	196.3068
F	9.1823*10^3

4.2 Performance in Case of BDEFG Fault: The performance of HHT is checked for BDEFG four phase to ground fault simulated at 40 km away from the relaying point at fault triggering time of 0.1 seconds with R_F = 4 Ω and R_G = 8 Ω. Figure 7 demonstrates the waveform of six phase current for BDEFG fault. Figure 8 depicts the Hilbert Huang transform coefficients of six phase current for BDEFG fault. Table 3 reports the response of HHT for BDEFG fault. From Table 3, it is inspected that the amplitudes of Hilbert Huang coefficients of the faulted phases are greater than the amplitudes of Hilbert Huang coefficients of the healthy phases. Therefore, it is clear from Table 3 that the HHT accurately detects the BDEFG fault.

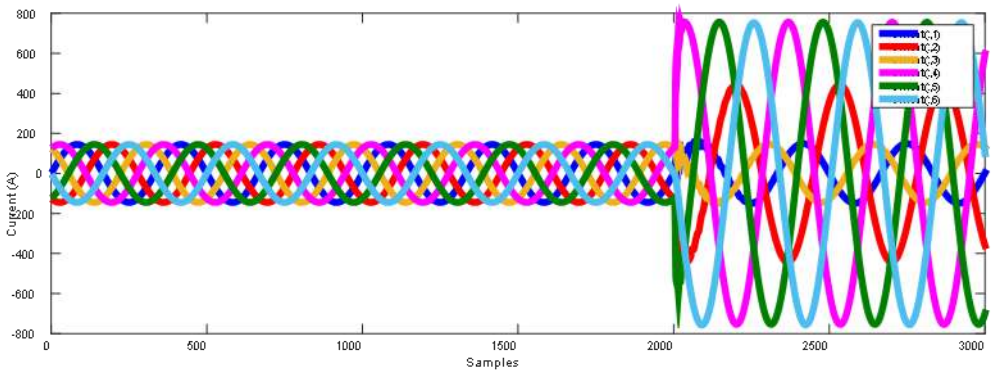

Figure 7. Six phase current for BDEFG fault at FIT=0.1 seconds with R_F = 4 Ω and R_G = 8 Ω

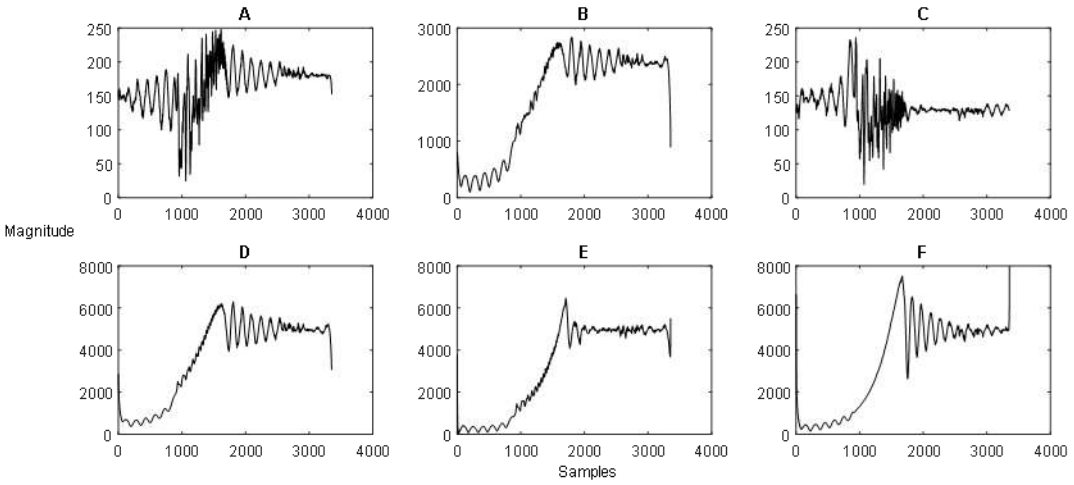

Figure 8. HHT coefficients of six phase current for BDEFG fault at FIT=0.1 seconds with R_F = 4 Ω and R_G = 8 Ω

Table 3. Result for BDEFG fault at 40 km at FIT = 0.1 seconds with R_F = 4 Ω and R_G = 8 Ω

Phase	Hilbert Huang Transform Coefficients
A	248.5096
B	2.8393*10^3
C	235.8718
D	6.2949*10^3
E	6.4717*10^3
F	7.9797*10^3

4.3 Performance in Case of ACDEG Fault: The response of HHT is investigated for ACDEG four phase to ground fault triggered at 45 km away from the relaying point at fault initiation time of 0.15 seconds with R_F = 6 Ω and R_G = 12 Ω. Figure 9 exemplifies the waveform of six phase current for ACDEG fault. Figure 10 depicts the Hilbert Huang coefficients of six phase current for ACDEG fault. Table 4 reports the result of HHT for ACDEG fault. From Table 4, it is clear that the amplitudes of Hilbert Huang coefficients of the faulted phases are larger than the amplitudes of Hilbert Huang coefficients of the healthy phases. Therefore, it is obvious from Table 4 that the HHT correctly detects the ACDEG fault.

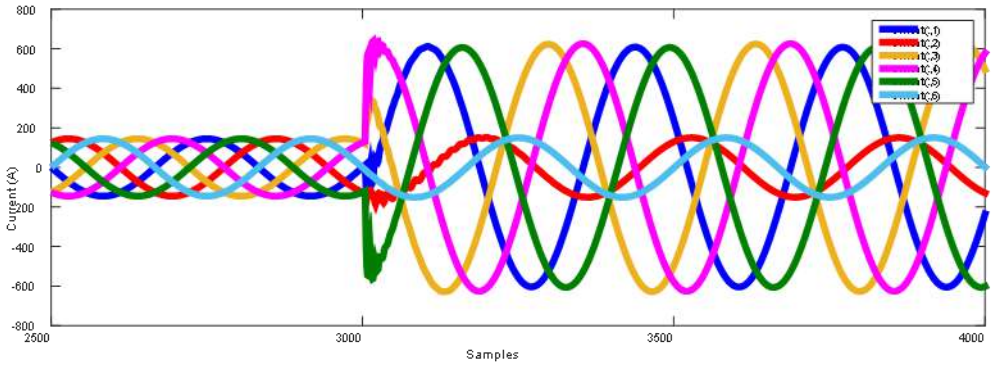

Figure 9. Six phase current for ACDEG fault at FIT=0.15 seconds with R_F = 6 Ω and R_G = 12 Ω

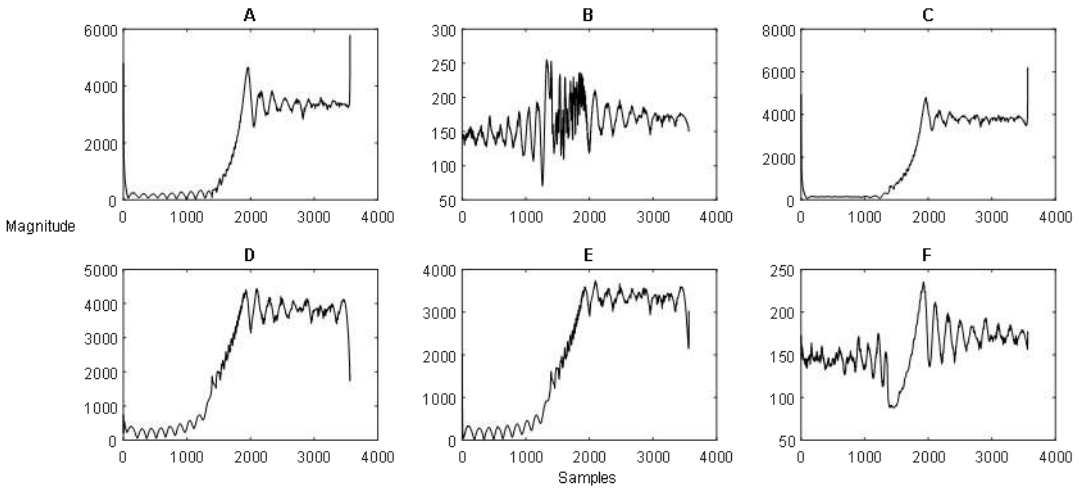

Figure 10. HHT coefficients of six phase current for ACDEG fault at FIT=0.15 seconds with R_F = 6 Ω and R_G = 12 Ω

Table 4. Result for ACDEG fault at 45 km at FIT= 0.15 seconds with R_F = 6 Ω and R_G = 12 Ω

Phase	Hilbert Huang Transform Coefficients
A	5.7847*10^3
B	255.0678
C	6.1936*10^3
D	4.4429*10^3
E	3.7413*10^3
F	235.1222

4.4 Performance in Case of BCEFG Fault: The performance of HHT is tested for BCEFG four phase to ground fault simulated at 5 km away from the relaying point at 0.02 seconds with R_F = 8 Ω and R_G = 16 Ω. Figure 11 illustrates the waveform of six phase current for BCEFG fault. Figure 12 depicts the Hilbert Huang coefficients of six phase current for BCEFG fault. Table 5 shows the response of HHT for BCEFG fault. From Table 5, it is seen that the amplitudes of Hilbert Huang coefficients of the faulted phases are larger than the amplitudes of Hilbert Huang coefficients of the healthy phases. Therefore, it is apparent from Table 5 that the HHT perfectly recognizes the BCEFG fault.

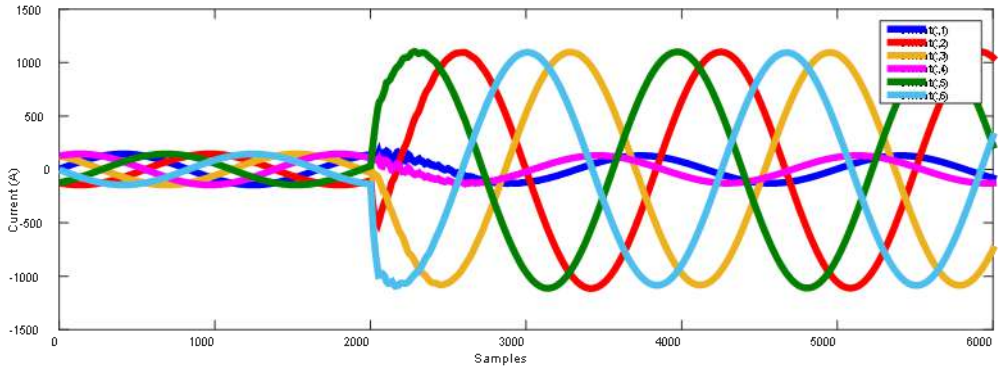

Figure 11. Six phase current for BCEFG fault at FIT=0.02 seconds with R_F = 8 Ω and R_G = 16 Ω

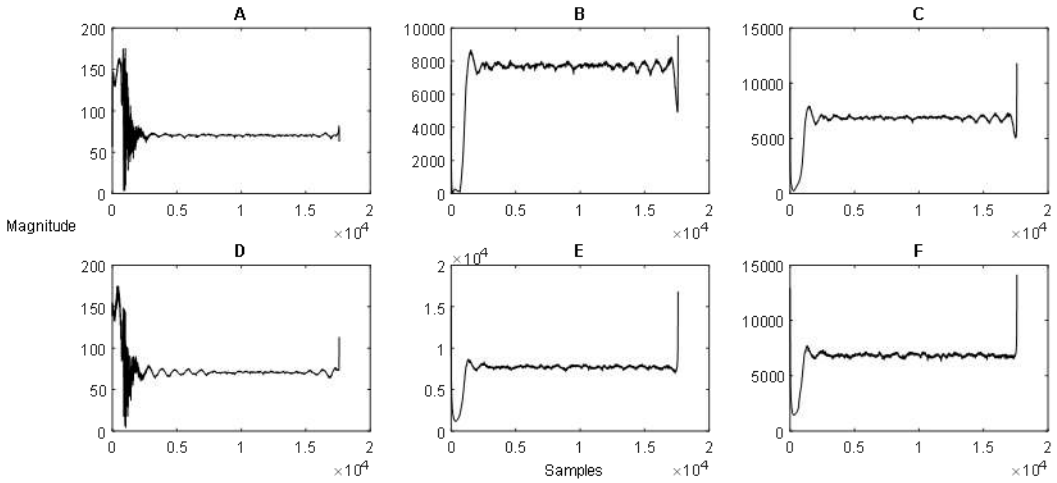

Figure 12. HHT coefficients of six phase current for BCEFG fault at FIT=0.02 seconds with R_F = 8 Ω and R_G = 16 Ω

Table 5. Result for BCEFG fault at 5 km at FIT= 0.02 seconds with R_F = 8 Ω and R_G = 16 Ω

Phase	Hilbert Huang Transform Coefficients
A	175.4154
B	9.5357*10^3
C	1.1778*10^4
D	174.8962
E	1.6790*10^4
F	1.4123*10^4

4.5 Performance in Case of CDEBG Fault: The performance of HHT is inspected for CDEBG four phase to ground fault triggered at 65 km away from the relaying point at 0.075 seconds with R_F = 10 Ω and R_G = 20 Ω. Figure 13 depicts the waveform of six phase current for CDEBG fault. Figure 14 shows the Hilbert Huang coefficients of six phase current for CDEBG fault. Table 6 reports the results of HHT for CDEBG fault. It is examined from Table 6 that the amplitudes of Hilbert Huang coefficients of the faulted phases are larger than the amplitudes of Hilbert Huang coefficients of the healthy phases. Hence, it is understandable from Table 6 that the HHT accurately detects the CDEBG fault.

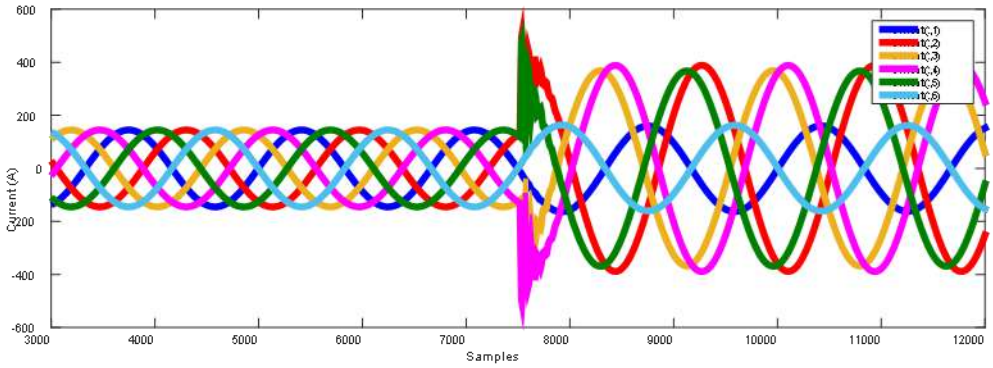

Figure 13. Six phase current for CDEBG fault at FIT=0.075 seconds with R_F = 10 Ω and R_G = 20 Ω

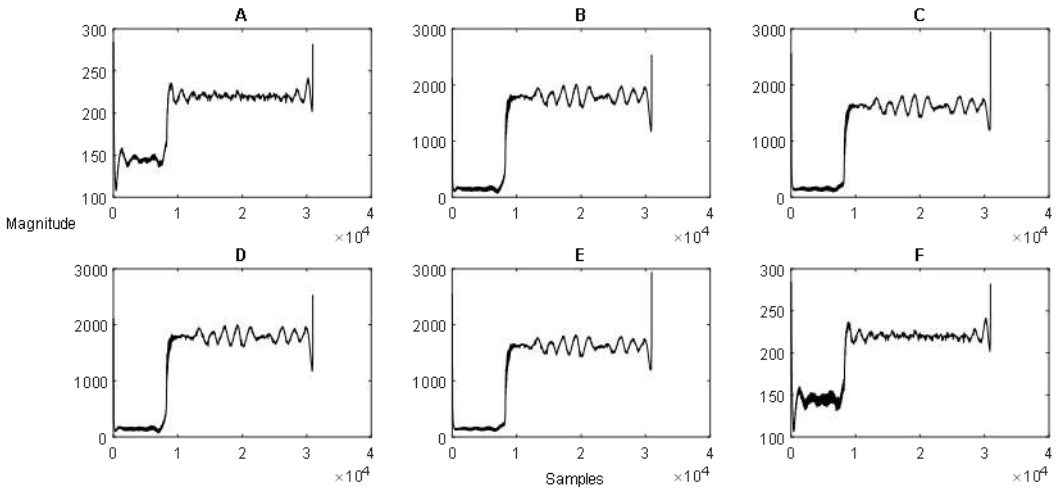

Figure 14. HHT coefficients of six phase current for CDEBG fault at FIT=0.075 seconds with R_F = 10 Ω and R_G = 20 Ω

Table 6. Result for CDEBG fault at 65 km at FIT=0.075 seconds with R_F = 10 Ω and R_G = 20 Ω

Phase	Hilbert Huang Transform Coefficients
A	284.1665
B	2.5383*10^3
C	2.9483*10^3
D	2.5313*10^3
E	2.9412*10^3
F	284.2040

4.6 Performance in Case of ABCDG Fault: The HHT is tested for ABCDG four phase to ground fault at 50 km away from the relaying point at 0.125 seconds with R_F = 12 Ω and R_G = 24 Ω. Figure 15 exemplifies the waveform of six phase current for ABCDG fault. Figure 16 depicts the Hilbert Huang coefficients of six phase current for ABCDG fault. Table 7 shows the result of HHT for ABCDG fault. It is clear from the results that the amplitudes of Hilbert Huang coefficients of the faulted phases are greater than the amplitudes of Hilbert Huang coefficients of the healthy phases. Hence, the HHT correctly recognizes the ABCDG fault.

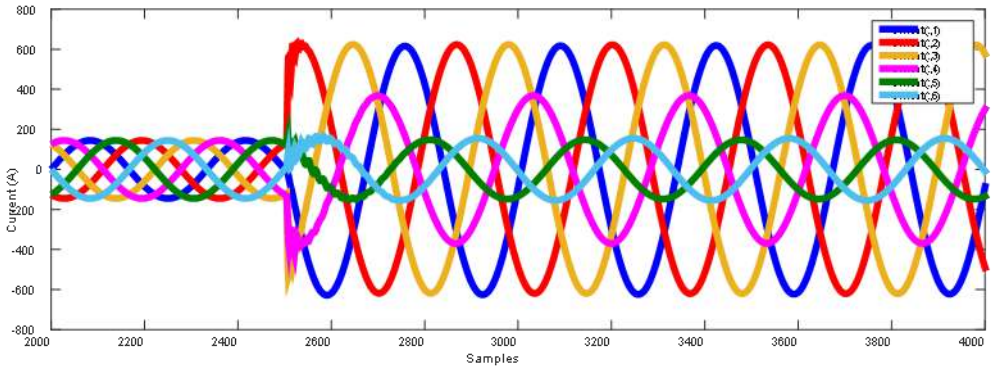

Figure 15. Six phase current for ABCDG fault at FIT=0.125 seconds with R_F = 12 Ω and R_G = 24 Ω

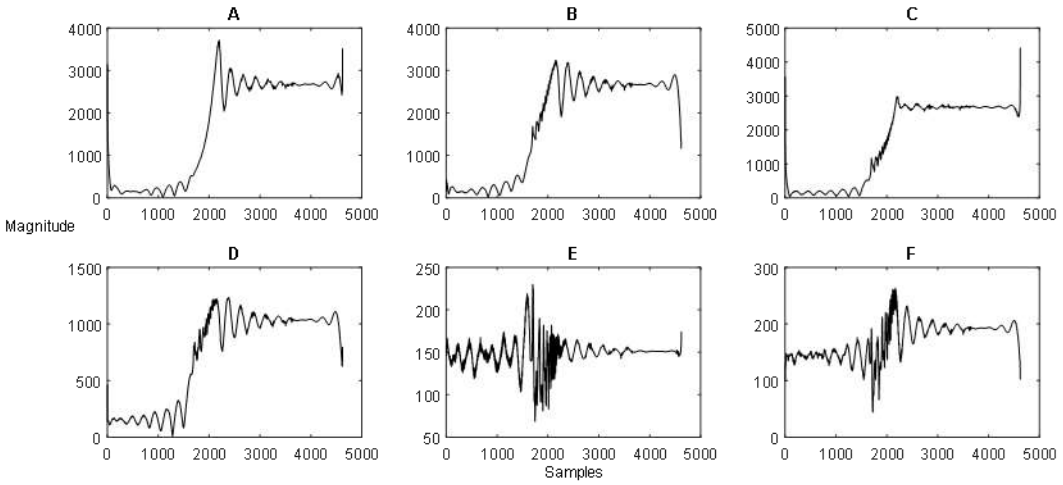

Figure 16. HHT coefficients of six phase current for ABCDG fault at FIT=0.125 seconds with R_F = 12 Ω and R_G = 24 Ω

Table 7. Result for ABCDG fault at 50 km at FIT=0.125 seconds with R_F= 12 Ω and R_G = 24 Ω

Phase	Hilbert Huang Transform Coefficients
A	3.7116*10^3
B	3.2429*10^3
C	4.4120*10^3
D	1.2360*10^3
E	229.8691
F	263.0660

4.7 Performance in Case of CDEFG Fault: The response of HHT is explored for CDEFG four phase to ground fault at 55 km away from the relaying point at 0.03 seconds with R_F = 14 Ω and R_G = 28 Ω. Figure 17 shows the waveform of six phase current for CDEFG fault. Figure 18 depicts the Hilbert Huang coefficients of six phase current for CDEFG fault. Table 8 exemplifies the results of HHT for CDEFG fault. It is seen from Table 8 that the amplitudes of Hilbert Huang coefficients of the faulted phases are greater than the amplitudes of Hilbert Huang coefficients of the healthy phases. Hence, the HHT perfectly detects the CDEFG fault.

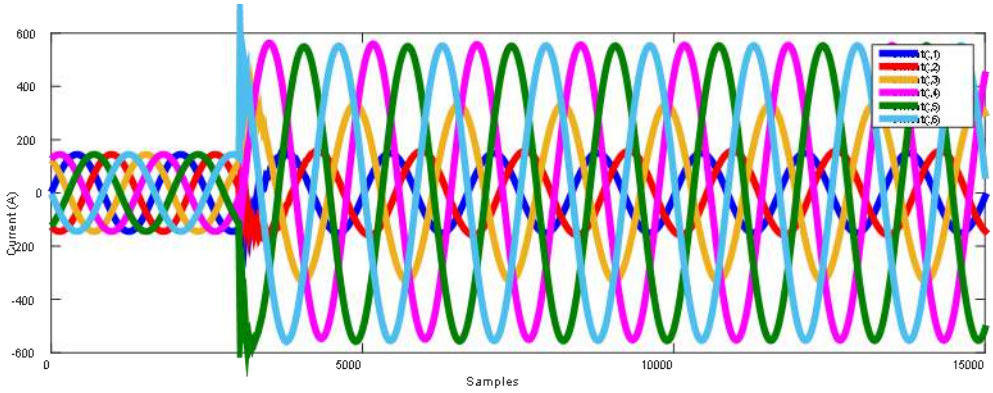

Figure 17. Six phase current for CDEFG fault at FIT=0.03 seconds with R_F = 14 Ω and R_G = 28 Ω

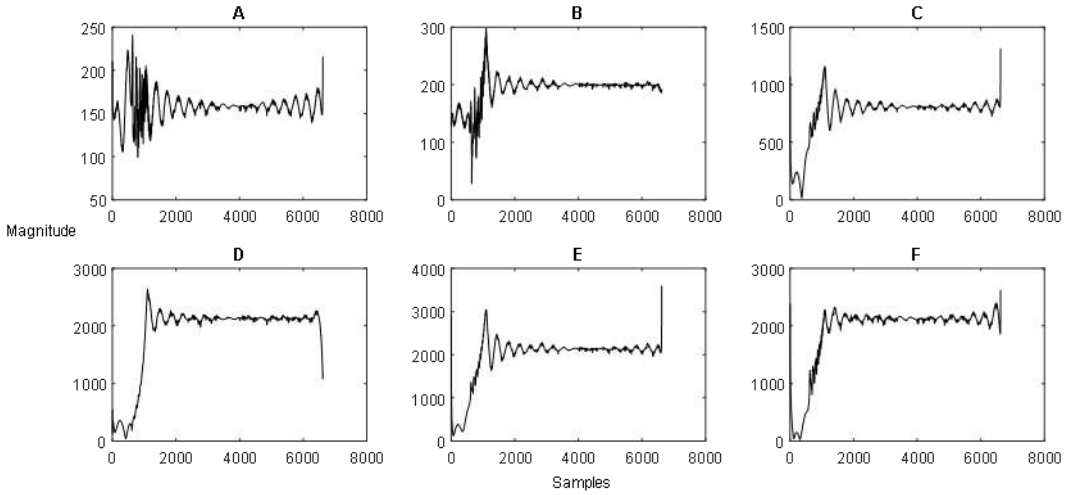

Figure 18. HHT coefficients of six phase current for CDEFG fault at FIT=0.03 seconds with R_F = 14 Ω and R_G = 28 Ω

Table 8. Result for CDEFG fault at 55 km at FIT=0.03 seconds with R_F = 14 Ω and R_G = 28 Ω

Phase	Hilbert Huang Transform Coefficients
A	241.0555
B	298.3368
C	1.3130*10^3
D	2.6431*10^3
E	3.5918*10^3
F	2.6187*10^3

5. Conclusion

The Hilbert Huang transform (HHT) is seemed to be very efficient under miscellaneous fault categories for the 138 kV six-phase transmission line. The HHT coefficients of the six-phase fault currents are estimated. The fault factors of the simulation model are varied and it is explored that the fault factors do not influence the reliability of the HHT. The results substantiates that the HHT has the capability to protect the six-phase transmission line besides various fault categories. The future work is planned on execution of the proposed technique on a digital platform (preferably digital signal processor) and assessing the scheme for more practical conditions.

References

Dubey R., Samantaray S. R., Panigrahi B. K., and Venkoparao V. G., 2018. Koopman analysis based wide-area back-up protection and faulted line identification for series-compensated power network, *IEEE Systems Journal*, Vol. 12, No. 3, pp. 2634-2644.

Gautam N., Ali S., and Kapoor G., 2018. Detection of fault in series capacitor compensated double circuit transmission line using wavelet transform, *Proc. IEEE Int. Conf. Computing, Power and Communication Technologies (GUCON)*, pp. 769-773.

Gautam N., Kapoor G., and Ali S., 2018. Wavelet transform based technique for fault detection and classification in a 400 kV double circuit transmission line, *Asian Journal of Electrical Sciences*, Vol. 7, No. 2, pp. 77-83.

Gaur V. K. and Bhalja B., 2017. New fault detection and localization technique for double-circuit three-terminal transmission line, IET Generation, Transmission and Distribution, Vol. 12, No. 8, pp. 1687-1696.

Guillen D., Paternina M. R. A., Bejar J. O., Tripathy R. K., Mendez A. Z., Olvera R. T., and Tellez E. S., 2018. Fault detection and classification in transmission lines based on a PSD index, *IET Generation, Transmission and Distribution*, Vol. 12, No. 18, pp. 4070-4078.

Geddada N., Yeap Y. M., and Ukil A., 2018. Experimental validation of fault identification in VSC-based DC grid system, *IEEE Transactions on Industrial Electronics*, Vol. 65, No. 6, pp. 4799-4809.

Govar S. A. and Seyedi H., 2016. Adaptive CWT-based transmission line differential protection scheme considering cross-country faults and CT saturation, *IET Generation, Transmission and Distribution*, Vol. 10, No. 9, pp. 2035-2041.

Hamidi R. J. and Livani H., 2017. Travelling wave-based fault location algorithm for hybrid multi-terminal circuits, *IEEE Transactions on Power Delivery*, Vol. 32, No. 1, pp. 135-144.

Jena M. K., Samantaray S. R., and Panigrahi B. K., 2017. A new wide-area backup protection scheme for series-compensated transmission system, *IEEE Systems Journal*, Vol. 11, No. 3, pp. 1877-1887.

Kapoor G., 2018. Wavelet transform based detection and classification of multi-location three phase to ground faults in twelve phase transmission line. *Majlesi Journal of Mechatronic Systems*, Vol. 7, No. 4, pp. 47-60.

Kapoor G., 2018. Six-phase transmission line boundary protection using wavelet transform. *Proceedings of the 8th IEEE India International Conference on Power Electronics (IICPE)*.

Kapoor G., 2018. Fault detection of phase to phase fault in series capacitor compensated six-phase transmission line using wavelet transform. *Jordan Journal of Electrical Engineering*, Vol. 4, No. 3, pp. 151-164.

Kapoor G., 2018. Six-phase transmission line boundary protection using mathematical morphology. *Proceedings of the IEEE International Conference on Computing, Power and Communication Technologies (GUCON)*, pp. 857-861.

Kapoor G., 2019. Detection and classification of single line to ground boundary faults in a 138 kV six phase transmission line using Hilbert Huang transform, *i-manager's Journal on Electrical Engineering*, Vol. 12, No. 3, pp. 28-41.

Kapoor G., 2019. Protection technique for series capacitor compensated three phase transmission line connected with distributed generation using discrete Walsh Hadamard transform, *International Journal of Engineering, Science and Technology*, Vol. 11, No. 3, pp. 1-10.

Kapoor G., 2018. A contemporary discrete wavelet transform based twelve phase series capacitor compensated transmission line protection, *International Journal of Engineering, Research and Technology*, Vol. 7, No. 5, pp. 263-271.

Kapoor G., 2018. Wavelet transform based fault detector for protection of series capacitor compensated three phase transmission line, *International Journal of Engineering, Science and Technology*, Vol. 10, No. 4, pp. 29-49.

Kapoor G., 2018. Discrete wavelet transform based technique to locate faults in three terminal transmission lines, *Journal of Advanced Research in Electrical Engineering and Technology*, Vol. 5, No. 3, pp. 1-8.

Kapoor G., 2018. A fault location evaluation method of a 330 kV three phase transmission line by using discrete wavelet transform, *International Journal of Engineering, Design and Analysis*, Vol. 1, No. 1, pp. 5-10.

Kapoor G., 2019. A protection technique for series capacitor compensated 400 kV double circuit transmission line based on wavelet transform including inter-circuit and cross-country faults, *International Journal of Engineering, Science and Technology*, Vol. 11, No. 2, pp. 1-20.

Kapoor G., 2018. Detection of phase to phase faults and identification of faulty phases in series capacitor compensated six phase transmission line using the norm of wavelet transform, *i-manager's Journal on Digital Signal Processing*, Vol. 6, No. 1, pp. 10-20.

Kapoor G., 2018. A discrete wavelet transform approach to fault location on a 138 kV two terminal transmission line using current signals of both ends, *ICTACT Journal of Microelectronics*, Vol. 4, No. 3, pp. 625-629.

Kapoor G., 2019. Detection and classification of three phase to ground faults in a 138 kV six-phase transmission line using Hilbert-Huang transform, *JEA Journal of Electrical Engineering*, Vol. 3, No. 1, pp. 1-11.

Kapoor G., 2018. Mathematical morphology based fault detector for protection of double circuit transmission line, *ICTACT Journal of Micro Electronics*, Vol.4, No.2, pp. 589-600.

Kapoor G., 2018. Wavelet transform based fault detector for protection of series capacitor compensated three phase transmission line, *International Journal of Engineering, Science and Technology*, Vol. 10, No. 4, pp. 29-49.

Kapoor G., 2018. Protection scheme for double circuit transmission lines based on wavelet transform, *ICTACT Journal of Micro Electronics*, Vol. 4, No. 3, pp. 656-664.

Koley E., Verma K., Ghosh S., 2015. An Improved Fault Detection, Classification and Location Scheme Based on Wavelet Transform and Artificial Neural Network for Six-phase Transmission Line using Single end Data Only. *Springer Plus*, Vol. 4, No. 1, pp. 1-22.

Ma Y., Li H., Wang G. and Wu J., 2018. Fault analysis and travelling-wave-based protection scheme for double-circuit LCC-HVDC transmission lines with shared towers, *IEEE Transactions on Power Delivery*, Vol. 33, No. 3, pp. 1479-1488.

Patel U. J., Chothani N. G., and Bhatt P. J., 2018. Sequence-space-aided SVM classifier for disturbance detection in series compensated transmission line, *IET Science, Measurement and Technology*, Vol. 12, No. 8, pp. 983-993.

Rajaraman P., Sundaravaradan N. A., Meyur R., Jaya Bharatha Reddy M., and Mohanta D. K., 2016. Fault classification in transmission lines using wavelet multi-resolution analysis, *IEEE Potentials*, Vol. 35, No. 1, pp. 38-44.

Saber A., Emam A., and Elghazaly H., 2017. A backup protection technique for three-terminal multi section compound transmission lines, *IEEE Transactions on Smart Grid*, Vol. 9, No. 6, pp. 5653-5663.

Sharma K., Ali S., and Kapoor G., 2017. Six-phase transmission line boundary fault detection using mathematical morphology. *International Journal of Engineering Research and Technology*, Vol. 6, No. 12, pp. 150-154.

Sharma P., Kapoor G., and Ali S., 2018. Fault detection on series capacitor compensated transmission line using Walsh Hadamard transform, *Proceedings of the IEEE International Conference on Computing, Power and Communication Technologies (GUCON)*, pp. 763-768.

Sharma N., Ali S. and Kapoor G., 2018. Fault detection in wind farm integrated series capacitor compensated transmission line using Hilbert Huang transform. *Proceedings of the IEEE International Conference on Computing, Power and Communication Technologies (GUCON)*, pp. 774-778.

Sharma P., Ali S., and Kapoor G., 2018. Wavelet transform approach for fault detection of three phase transmission line compensated with series capacitor, *Asian Journal of Electrical Sciences*, Vol. 7, No. 2, pp. 8-13.

Biographical notes

Gaurav Kapoor received B.E. in Electrical Engineering from University of Rajasthan, Jaipur, India and M. Tech. in Power System specialization from University College of Engineering, Rajasthan Technical University, Kota, India in 2011 and 2014, respectively. He is an Assistant Professor in the Department of Electrical Engineering, Modi Institute of Technology Kota, India. He has published more than forty five papers in various journals. He has also presented many research papers in national and international conferences. His research interests include power system digital protection.

Received December 2018
Accepted June 2019
Final acceptance in revised form July 2019